Steady Heat and Mass Transfer by Mixed Convection Flow from a Vertical Porous Plate with Induced Magnetic Field, Constant Heat and Mass Fluxes

Md. Mahmud Alam*
Mathematics Discipline; Science, Engineering and Technology School
Khulna University, Khulna-9208, Bangladesh
Mohammad Rafiqul Islam
Mathematics Department, Ahsanullah University of Science & Technology
Rajshahi Campus, Talaimary, Rajshahi, Bangladesh
Fouzia Rahman
Mathematics Department, Khulna University of Engineering & Technology, Khulna-9203, Bangladesh

Abstract

Steady heat and mass transfer by mixed convection flow from a vertical porous plate with constant heat and mass fluxes has been studied under the action of transverse applied magnetic field taking into account the induced magnetic field. The boundary layer equations have been transformed into dimensionless coupled nonlinear ordinary differential equations by appropriate transformations. The similarity solutions of the transformed dimensionless equations for the flow field, induced magnetic field, current density, heat and mass transfer characteristics are obtained by shooting iteration technique. Numerical results are presented in the form of velocity, induced magnetic field, current density, and temperature and concentration distributions within the boundary layer for different parameters entering into the analysis. Finally, the effects of the pertinent parameters on the skin-friction coefficient and current density at the plate are also examined.

Keywords: Mixed convection, Induced magnetic field, Current density, Constant heat and mass fluxes.

1. Introduction

Magnetohydrodynamics (MHD) is currently undergoing a period of great enlargement and differentiation of subject matter. The science of magnetohydrodynamics was concerned with geophysical and astrophysical problems for a number of years. In recent years the possible use of MHD is to affect a flow stream of an electrically conducting fluid for the purpose of thermal protection, braking, propulsion and control. From the point of applications, several investigators have made model studies on the effect of magnetic field on free convection flows. Some of them are Georgantopoulos[1], Nanousis et al.[2] and Raptis and Singh[3]. Along with the effects of magnetic field, the effect of transpiration parameter, being an effective method of controlling the boundary layer, has been considered by Kafoussias[4] and Singh[5]. Singh et al. [6] studied magnetohydrodynamics heat and mass transfer flow of a viscous incompressible fluid past an infinite vertical porous plate under oscillatory suction velocity normal to the plate. The combined heat and mass transfer of an electrically conducting fluid in MHD natural convection adjacent to a vertical surface was analyzed by Chen [7].

All the above works are related to the stationary vertical surface. However, the flow past a continuously moving surface has many applications in manufacturing processes such as hot rolling, metal and plastic extrusion, continuous casting, and glass fiber and paper production. Sakiadis [8, 9] was the first author to recognize this backward boundary-layer situation and used a similarity transformation to obtain a numerical solution for the flow field of a continuously moving surface. The heat transfer

*Corresponding author;
email:alam_mahmud2000@yahoo.com

flow past a continuous moving plate with variable temperature was investigated by Soundalgekar and Ramana Murty[10]. Sami A. Al-Sanea[11] studied the steady laminar flow and heat transfer characteristics of a continuously moving vertical sheet of extruded material. Quite recently an analytical study of the one dimensional steady combined heat and mass transfer by mixed convection flow of an incompressible electrically conducting viscous fluid past an electrically non-conducting continuously moving infinite vertical porous plate under the action of a strong magnetic field with constant suction velocity, constant heat and mass fluxes was done by Chaudhary and Sharma [12]. The level of concentration of foreign mass was assumed to be very low in this study so that the thermal and mass diffusion were neglected. They used a perturbation technique to obtain the solution and did not show the complete results due to some analytical restrictions.

Along with these studies, the effect of thermal diffusion on MHD free convection and mass transfer flows have also been considered by many investigators due to its important role particularly in isotope separation and in mixtures between gases with very light molecular weight (H_2, H_e) and medium molecular weight (N_2, air) (Eckert and Drake, [13]). Considering these aspects, model studies were carried out by many investigators of whom the names of Kafoussias[14], Nanousis[15], Sattar and Alam[16] and Alam et al. [17] are worth mentioning. Recently both Soret and Dufour effects on steady mixed convection flow past a semi-infinite vertical porous flat plate in a porous medium with variable suction was investigated by Alam and Rahman[18].

In all the papers cited earlier, the studies concentrated on MHD free convection and mass transfer flow of an incompressible viscous fluid under only the action of transverse magnetic field with or without thermal and mass diffusions.

The present study, therefore, extends the work of Chaudhary and Sharma [12] investigating steady MHD heat and mass transfer by mixed convection flow from a moving vertical porous plate with induced magnetic, thermal diffusion, constant heat and mass fluxes. The governing equations of the problem contain the partial differential equations, which are transformed by similarity transformation into a system of ordinary coupled non-linear differential equations. The obtained ordinary coupled non-linear differential equations are solved numerically by sixth order Runge Kutta method along with the Nachtsheim-Swigert[19] iteration technique. The complete obtained results are shown graphically as well as in tabular form.

2. The Governing Equations

Let us consider a steady MHD heat and mass transfer flow of an electrically conducting viscous fluid past an infinite vertical porous plate $y=0$ which is impulsively started with velocity U_0. The flow is also assumed to be in the x direction, which is taken along the plate in upward direction, and y-axis is normal to it. The constant heat flux $\left(-k\frac{\partial T}{\partial y}\right)= q$ and constant species mass flux $\left(-D_m\frac{\partial C}{\partial y}\right)= m$ at the plate are considered, where D_m is the coefficient of mass diffusion and k is the thermal conductivity. T and T_∞ are the fluid temperature within the boundary layer and the fluid temperature in the free stream respectively, while C and C_∞ are the corresponding concentrations. We assumed that the magnetic Reynolds number of the flow is large enough so that the induced magnetic field is not negligible. The induced magnetic field is of the form $\mathbf{H}=(H_x, H_0, 0)$. A uniform magnetic field strength H_0 is applied to the plate, acting along the y-axis, which is electrically non-conducting. The level of concentration of foreign mass is assumed high so that the thermal diffusion is considered. The equation of the conservation of electric charge is $\nabla\cdot\mathbf{J}=0$, where $\mathbf{J}=(J_x, J_y, J_z)$. The direction of propagation is considered only along the y-axis and does not have any variation along the y-axis and the derivative of **J** with respect to y is namely $\frac{\partial J_y}{\partial y}=0$, resulting in $J_y=$constant. Since the plate is electrically non-conducting, this constant is zero and hence $J_y=0$ everywhere in the flow. The flow configuration and coordinate system are shown in Fig.1. It is assumed that the plate is semi-infinite in extent and hence all the physical quantities depend on y and x. Thus,

inaccordance with the above assumptions and Boussinesq's approximation, the basic equations relevant to the problem are:

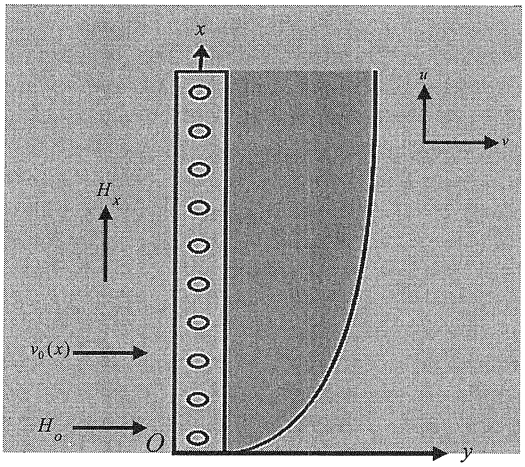

Fig. 1. Physical configuration and coordinate system.

$$\frac{\partial u}{\partial x}+\frac{\partial v}{\partial y}=0 \tag{1}$$

$$u\frac{\partial u}{\partial x}+v\frac{\partial u}{\partial y}=g\beta(T-T_\infty)+g\beta^*(C-C_\infty)+\upsilon\frac{\partial^2 u}{\partial y^2}+\frac{\mu_e}{\rho}H_o\frac{\partial H_x}{\partial y} \tag{2}$$

$$u\frac{\partial H_x}{\partial x}+v\frac{\partial H_x}{\partial y}=H_x\frac{\partial u}{\partial x}+H_o\frac{\partial u}{\partial y}+\frac{1}{\mu_e\sigma'}\frac{\partial^2 H_x}{\partial y^2} \tag{3}$$

$$u\frac{\partial T}{\partial x}+v\frac{\partial T}{\partial y}=\frac{k}{\rho c_p}\frac{\partial^2 T}{\partial y^2}+\frac{\upsilon}{c_p}\left(\frac{\partial u}{\partial y}\right)^2+\frac{1}{\rho c_p\sigma'}\left(\frac{\partial H_x}{\partial y}\right)^2 \tag{4}$$

$$u\frac{\partial C}{\partial x}+v\frac{\partial C}{\partial y}=D_m\frac{\partial^2 C}{\partial y^2}+\frac{D_m K_T}{T_m}\frac{\partial^2 T}{\partial y^2} \tag{5}$$

and the boundary conditions for the problem are

$$\left.\begin{aligned} &u=U_o, v=v_0(x), \frac{\partial T}{\partial y}=-\frac{q}{k}, \frac{\partial C}{\partial y}=-\frac{m}{D_m},\\ &H_x=H_w \text{ at } y=0\\ &u=0, T\to T_\infty, \quad C\to C_\infty, \quad H_x\to 0\\ &\text{as} \quad y\to\infty \end{aligned}\right\} \tag{6}$$

where all physical quantities are defined in the nomenclature and other symbols have their usual meaning.

3. Mathematical Formulations

To solve the above system of equations (1)-(5) under the boundary conditions (6) we adopt the well-defined similarity technique to obtain the similarity solutions.

For this purpose the following non-dimensional variables are introduced:

$$\eta=y\sqrt{\frac{U_o}{2\upsilon x}} \tag{7}$$

$$f'(\eta)=\frac{u}{U_o} \tag{8}$$

$$\theta(\eta)=\frac{k(T-T_\infty)}{q}\sqrt{\frac{U_o}{2\upsilon x}} \tag{9}$$

$$\phi(\eta)=\frac{D_m(C-C_\infty)}{m}\sqrt{\frac{U_o}{2\upsilon x}} \tag{10}$$

$$H(\eta)=\sqrt{\frac{\mu_e}{\rho}}\sqrt{\frac{2x}{U_o\upsilon}}H_x \tag{11}$$

Now from equations (1) and (8), we have

$$v=\sqrt{\frac{U_o\upsilon}{2x}}\left[\eta f'(\eta)-f(\eta)\right] \tag{12}$$

Also we have, $f_w=-v_0(x)\sqrt{\frac{2x}{U_o\upsilon}}$, (13)

where f_w is the suction parameter or transpiration parameter and the variables are defined in the nomenclature.

From equations (2) - (13), we have the following dimensionless ordinary coupled non-linear differential equations:

$$f'''+ff''+G_r\theta+G_m\phi+MH'=0 \tag{14}$$

$$H''+P_m(f'H+fH')-P_m\eta Hf''+MP_m f''=0 \tag{15}$$

$$\phi''+S_c(f\phi'-f'\phi)+S_oS_c\theta''=0 \tag{17}$$

with the corresponding boundary conditions:

$$\left.\begin{aligned} &f=f_w, f'=1, \theta'=-1, \phi'=-1, H=h=1\\ &\qquad\qquad\qquad\qquad\qquad\qquad \text{(say) at } \eta=0\\ &f'=0, \theta\to 0, \phi\to 0, H\to 0 \text{ as } \eta\to\infty \end{aligned}\right\} \tag{18}$$

where,

$G_r=g\beta\frac{q}{k}\sqrt{\frac{\upsilon(2x)^3}{U_o^5}}$ is the Grashof number,

$$G_m = g\beta^{\bullet}\frac{m}{D_m}\sqrt{\frac{\upsilon(2x)^3}{U_o{}^5}}$$

is the Modified Grashof number,

$$M = \sqrt{\frac{\mu_e}{\rho}}\frac{H_o}{U_o}$$

is the magnetic force number.

$$P_m = \mu_e\sigma'\upsilon$$

is the magnetic diffusivity number,

$P_r = \dfrac{\rho c_p \upsilon}{k} = \dfrac{\mu c_p}{k}$ is the Prandtl number,

$E_c = \dfrac{kU_o{}^2}{qc_p}\sqrt{\dfrac{U_o}{2\upsilon x}}$ is the Eckert number,

$S_o = \dfrac{qD_m^2 K_T}{k\upsilon m T_m}$ is the Soret number,

and $S_c = \dfrac{\upsilon}{D_m}$ is the Schmidt number.

In all the above equations primes denote the differentiation with respect to η.

4. Skin Friction Co-efficient and Current Density at the Plate

The skin friction coefficient and the Current density at the plate are the quantities of chief physical interest.

The shearing stress at the plate is generally known as the skin friction, the equation defining the skin friction is:

$$\tau = \mu\left(\frac{\partial u}{\partial y}\right)_{y=0} \quad i.e. \quad \tau \propto f''(0)$$

The current density is generally expressed as: $J = \left(-\dfrac{\partial H_x}{\partial y}\right)$ and hence the current density at the plate is $J_w \propto H'(0)$.

The next section deals with the solution technique of the problem.

5. Numerical Solution

The set of ordinary coupled non-linear differential equations (14)-(17) with the boundary conditions (18) for steady case are very difficult to solve analytically; so numerical procedures are adopted to obtain their solution. Here we use the standard initial value solver, namely the sixth order Runge Kutta method along with Nachtsheim-Swigert iteration technique.

In a Nachtsheim-Swigert iteration technique, the missing (unspecified) initial condition at the initial point of the interval is assumed and the differential equation is then integrated numerically as an initial value problem to the terminal point. The accuracy of the assumed missing initial condition is then checked by comparing the calculated value of the dependent variable at the terminal point with its given value there. If a difference exists, another value of the missing initial condition must be assumed and the process is repeated. This process in continued until the agreement between the calculated and the given condition at the terminal point is within the specified degree of accuracy. For this type of iterative approach, one naturally inquires whether or not there is a systematic way of finding each succeeding (assumed) value of the missing initial condition.

The Nachtsheim-Swigert iteration technique thus needs to be discussed elaborately. The boundary conditions (18) associated with the non-linear coupled ordinary differential equations (14)-(17) of the boundary layer type is of two point asymptotic classes. Two point boundary conditions have values of the dependent variable specified at two different values of independent variable. Specification of asymptotic boundary conditions implies that the first derivative (and higher derivatives of the boundary layer equations, if they exist) of the dependent variable approaches zero, and the value of the velocity approaches unity, as the other specified value of the independent variable is approached. The method of numerical integration of two point asymptotic boundary value problem of the boundary layer type, the initial value method, requires that the problem be recast as an initial value problem. Thus it is necessary to set up as many boundary conditions as the surfaces there at infinity. The governing differential equations are then integrated with these assumed surface boundary conditions. If the required outer boundary conditions are satisfied, a solution has been achieved. However, this is not generally the case. Hence, a method must be devised to logically estimate the new surface boundary conditions for the next trial integration. Asymptotic boundary value problems such as those governing boundary layer equations become more complicated by the fact that the outer boundary condition is

specified at infinity. In the trial integration, infinity is numerically approximated by some large value of the independent variable. There is no general method of estimating this value. Selecting too small a maximum value for the independent variable may not allow the solution to asymptotically converge to the required accuracy. Selecting a large value may result in slow convergence or even divergence of the trial integration. Selecting too large a value of the independent variable is expensive in terms of computer time. Nachtsheim-Swigert developed an iteration method, which overcomes these difficulties. Extensions of the Nachtsheim-Swigert iteration to the above system of differential equations (14)–(17) with boundary conditions are straightforward. In equation (18), there are four asymptotic boundary conditions and hence there will be four unknown surface conditions $f''(0)$, $H'(0)$, $\theta(0)$, $\phi(0)$.

6. Results and Discussion

The numerical values of the velocity, induced magnetic field, current density, temperature, the concentration skin friction and current density at the plate, respectively, for different values of the suction parameter (f_w), the magnetic parameter (M), the Prandtl number (P_r), the Soret number (S_o), the Schmidt number (S_c), the Grashof number (G_r), the magnetic diffusivity parameter (P_m), the Eckert number (E_c) and for the fixed values of modified Grashof number (G_m) are obtained and discussed. The values of M and G_r are taken to be large for a cooling Newtonian fluid, since these large values correspond to a strong magnetic field and to a cooling problem that is generally encountered in nuclear engineering in connection with the cooling of reactors.

The most important fluids are atmospheric air and water and so the results are limited for Prandtl number P_r=0.71 and 7.00 (in particular, 0.71 represents air at 20^{0}C and 7.0 corresponds to water at 20^{0}C). The value 0.60 is also considered for S_c, which represents the specific condition of the flow (0.60 corresponds to water vapor that represents a diffusivity chemical species of most common interest in air). The values of f_w, M, S_o, P_m, E_c and G_m are however chosen arbitrarily.

The obtained results are illustrated in Figs. (2)-(26) in case of air (P_r=0.71) and water (P_r=7.0). The plots of velocity, the induced magnetic field, current density, temperature and concentration versus η are shown in Figs. (2)-(6), (7)-(11), (12)-(16), (17)-(21) and (22)-(26) respectively for different value of f_w, M, P_m, S_o, and E_c.

The effect of the suction parameter f_w on the velocity is shown in Fig. (2). It is observed from this figure that an increase in f_w leads to a decrease in velocity in case of air (P_r=0.71) and water (P_r=7.0). The usual stabilizing effect of the suction parameter on the boundary layer growth is also evident from this figure. We also notice that for any value of f_w the velocity of air is greater than the velocity of water. The velocity profiles are shown in Figs. (3) and (4) for different values of M and P_m. It is observed that an increase in the applied magnetic field parameter and magnetic diffusivity parameter leads to an increase in the velocity within the domain $0<\eta<0.7$ and $0<\eta<0.4$, respectively, for both air and water. Further it is observed from these figures that the velocity distribution decreases gradually at the points where $\eta \geq 0.7$ and $\eta \geq 0.4$, respectively, for both air and water. Figs. (5)-(6) show the velocity profiles for different values of S_o, and E_c. We notice that an increase in S_o, and E_c leads to a rise in the values of the velocity for both air and water.

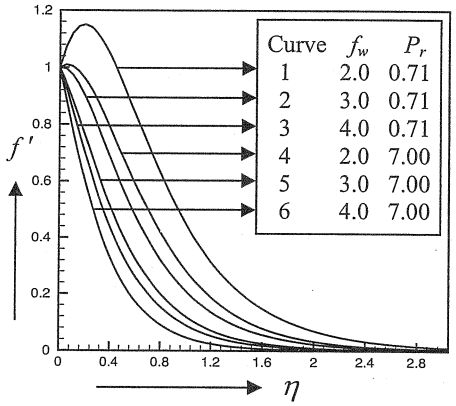

Fig. 2. Velocity profiles (f') for different values of f_w , taking G_r=5.0,G_m=2.0, M=1.0, P_m=1.0, S_o =2.0, S_c=0.6 and E_c=0.2 as fixed.

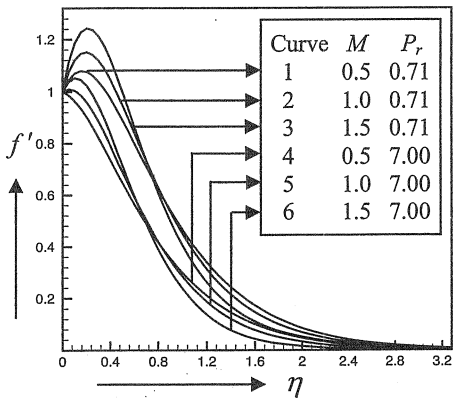

Fig. 3. Velocity profiles (f') for different values of M, taking f_w=2.0, G_r=5.0, G_m=2.0, P_m=1.0, S_o =2.0, S_c=0.6 and E_c=0.2 as fixed.

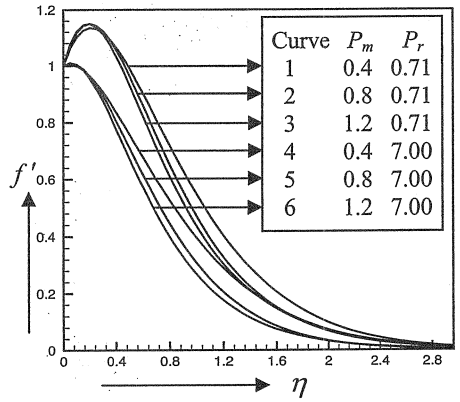

Fig. 4. Velocity profiles (f') for different values of P_m, taking f_w=2.0 , G_r=5.0, G_m=2.0, M=1.0, S_o =2.0, S_c=0.6 and E_c=0.2 as fixed.

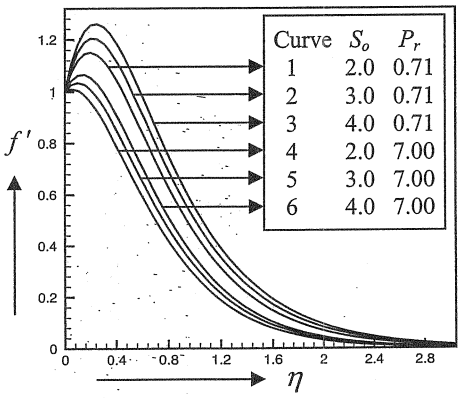

Fig. 5. Velocity profiles (f') for different values of S_o taking f_w=2.0 , G_r=5.0, G_m=2.0, M=1.0, P_m=1.0, S_c=0.6 and E_c=0.2 as fixed.

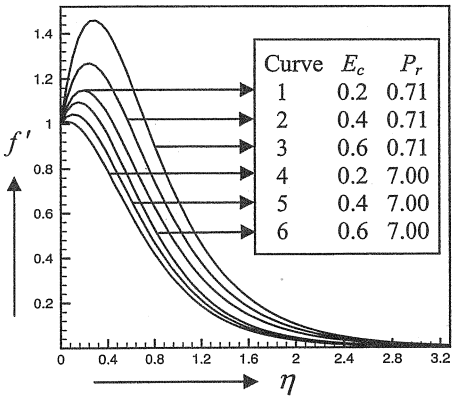

Fig. 6. Velocity profiles (f') for different values of E_c, taking f_w=2.0, G_r=5.0, G_m=2.0, M=1.0, P_m=1.0, S_o =2.0 and S_c=0.6 as fixed.

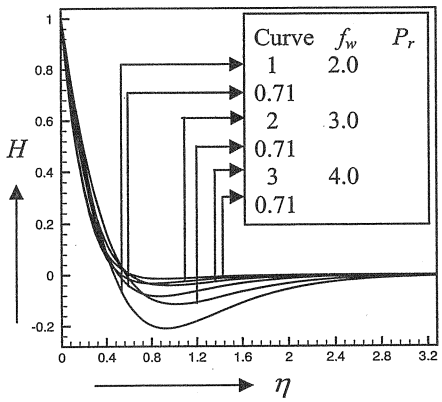

Fig. 7. Induced magnetic field (H) for different values of f_w , taking G_r=5.0, G_m=2.0, M=1.0, P_m=1.0, S_o =2.0, S_c=0.6 and E_c=0.2 as fixed.

Figs.(7)-(11) present the induced magnetic field for air (P_r=0.71) and water (P_r=7.0) respectively for different values of f_w, M, P_m, S_o, and E_c. It is observed from Fig. (7) that the induced magnetic field decreases a little within the interval $0 \le \eta \le 0.4$ with an increase in suction parameter (f_w) for both air and water, but it increases within the interval $0.4 \le \eta \le 2.0$ with an increase in f_w for both air and water. It is further observed that in the case of air for the interval $0.4 < \eta < 2.0$, H remains negative. It is observed from Figs. (8) and (9) that the induced magnetic field decreases with the increase of M and P_m for both air and water. It is also found

from these figures that the decrease effect is large. However, it has a negative value approximately in the interval ($0.4 \le \eta \le 2.4$). We thus may conclude that the transverse magnetic field and magnetic field diffusivity have a strong role on the induced magnetic field. It is observed from Figs. (10)-(11) that the induced magnetic field decreases with the increase of S_o, and E_c in case of air and water. The decreasing effect is not so prominent near the plate. In these figures, it appears that there is a back directional induced magnetic field in a considerable area of the boundary layer (approximately $0.4 \le \eta \le 2.4$).

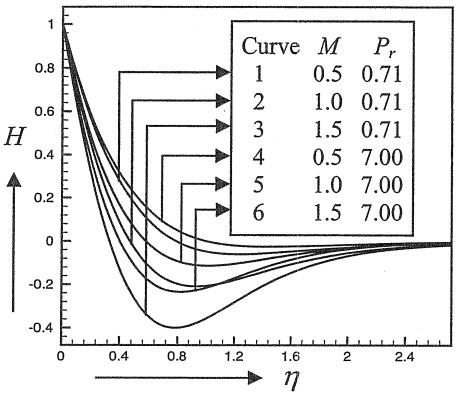

Fig. 8. Induced magnetic field (H) for different values of M, taking f_w=2.0, G_r=5.0,G_m=2.0, P_m=1.0, S_o =2.0, S_c=0.6 and E_c=0.2 as fixed.

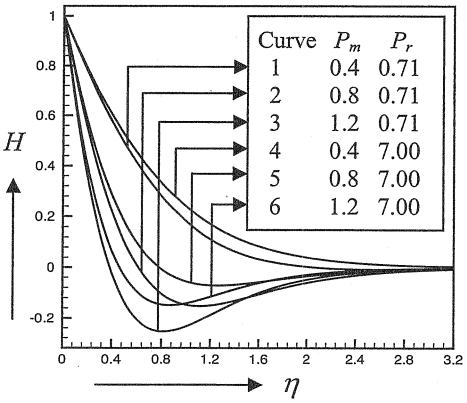

Fig. 9. Induced magnetic field (H) for different values of P_m, taking f_w=2.0 , G_r=5.0, G_m=2.0, M=1.0, S_o =2.0, S_c=0.6 and E_c=0.2 as fixed.

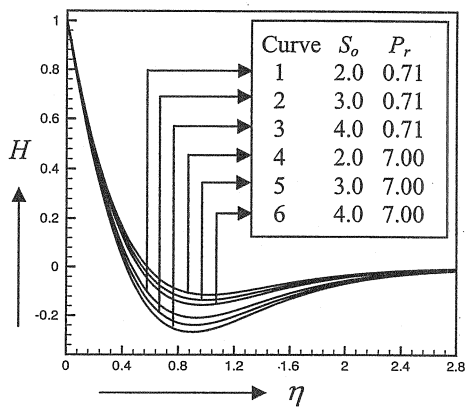

Fig. 10. Induced magnetic field (H) for different values of S_o taking f_w=2.0 , G_r=5.0, G_m=2.0, M=1.0, P_m=1.0, S_c=0.6 and E_c=0.2 as fixed.

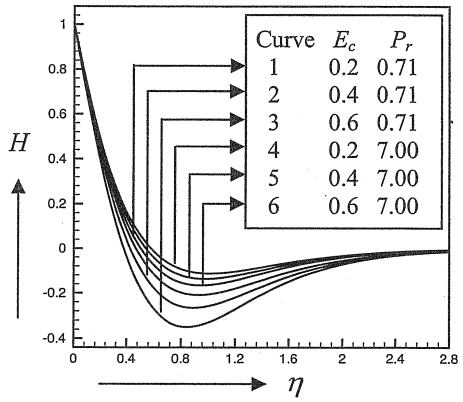

Fig. 11. Induced magnetic field (H) for different values of E_c, taking f_w=2.0, G_r=5.0, G_m=2.0, M=1.0, P_m=1.0, S_o =2.0 and S_c=0.6 as fixed.

Figs.(12)-(16) present the current density profiles for air (P_r=0.71) and water (P_r=7.0) for different values of f_w, M, P_m, S_o and E_c. In Fig. (12), it is observed that the current density increases approximately in the domain $0 < \eta < 0.17$, and further decreases in the interval $0.17 < \eta < 1$ with the increase of f_w, for both air and water. From the point where $\eta \ge 1$, it is reduced to a certain value of η and becomes constant. Fig. (13) shows that the current density increases in the interval $0 < \eta < 0.6$ (approx.) and decreases when $\eta > 0.6$ for both air and water with increase in M. It is

observed from Fig.(14) that the current density increases close to the plate within the interval $0 \le \eta \le 0.6$ (approx.). This increasing effect is very large. From the point where $\eta \ge 0.6$, current density decreases with the increase of P_m in both air and water (P_r=0.71 & 7.0). Fig.(15) shows the minor increasing/decreasing effect of the current density for different values of S_o for air and water. The effect is reversed after $\eta \approx 0.72$. Fig.(16) shows the increase of the current density in the interval $0 < \eta < 0.7$ and the decrease from $\eta > 0.7$ with increase of E_c for air and water.

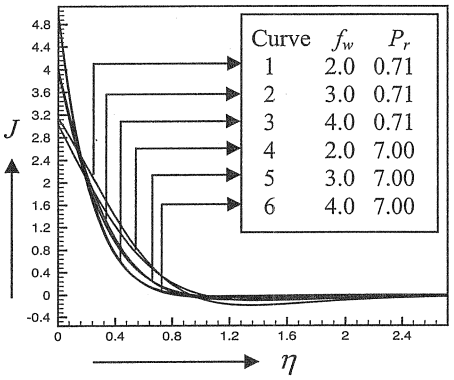

Fig. 12. Current density profiles (J) for different values of f_w , taking G_r=5.0, G_m=2.0, M=1.0, P_m=1.0, S_o =2.0, S_c=0.6 and E_c=0.2 as fixed.

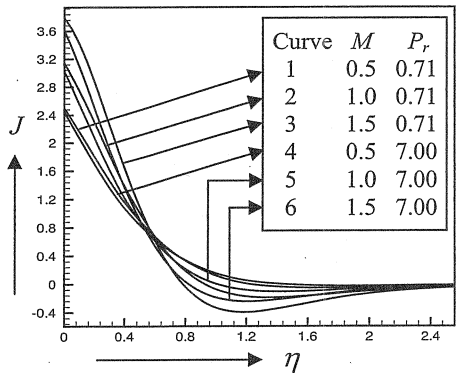

Fig. 13. Current density profiles (J) for different values of M, taking f_w=2.0, G_r=5.0, G_m=2.0, P_m=1.0, S_o =2.0, S_c=0.6 and E_c=0.2 as fixed.

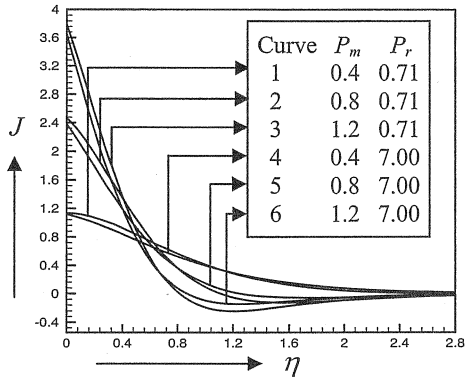

Fig. 14. Current density profiles (J) for different values of P_m, taking f_w=2.0 , G_r=5.0, G_m=2.0, M=1.0, S_o =2.0, S_c=0.6 and E_c=0.2 as fixed.

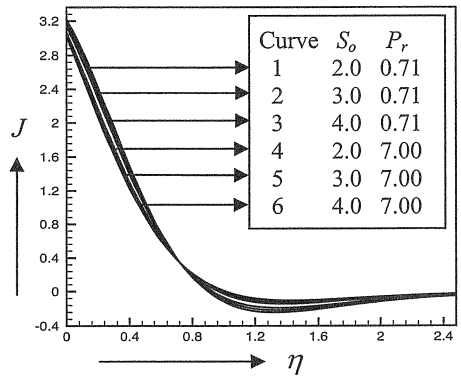

Fig. 15. Current density profiles (J) for different values of S_o, taking f_w=2.0 ,G_r=5.0, G_m=2.0, M=1.0, P_m=1.0, S_c=0.6 and E_c=0.2 as fixed.

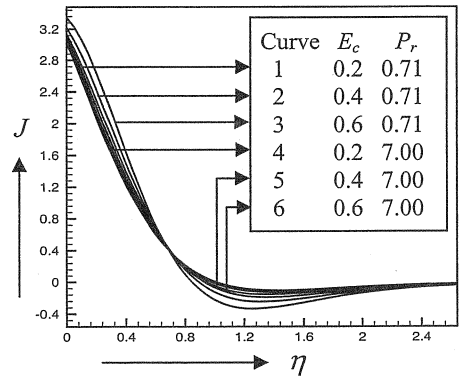

Fig. 16. Current density profiles (J) for different values of E_c, taking f_w=2.0, G_r=5.0, G_m=2.0, M=1.0, P_m=1.0, S_o =2.0 and S_c=0.6 as fixed.

The temperature profiles are shown in Figs. (17)-(21) for different values of f_w, M, P_m, S_o and E_c for both air (P_r=0.71) and water (P_r=7.0). It is observed from Fig. (17) that the temperature has a decreasing effect with increase in suction parameter (f_w) for both air and water. From Fig. (18), it is observed that the temperature increases as M increases for both air and water. Fig. (19) shows that there is a minor increasing effect of the temperature for increasing values of P_m in case of air; for water the temperature increases within the interval ($0<\eta<0.23$ approx.) and it decreases from $\eta>0.23$ with increase in P_m. Also it is found from Fig.(20) that the temperature distribution has a negligible effect with the increase of S_o, for both air and water. Fig. (21) shows that the temperature has a very large increasing effect close to the plate with the increase of E_c for both air and water. It is interesting to note that the temperature profiles are more sensitive for air (P_r=0.71) than for water (P_r=7.00).

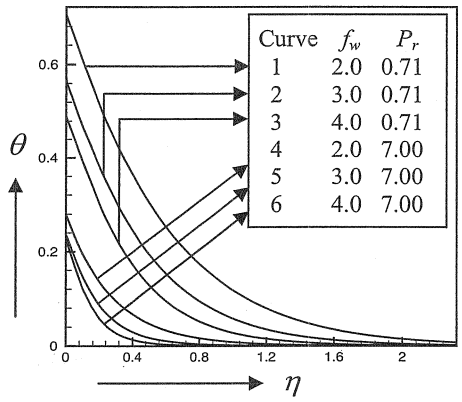

Fig. 17. Temperature profiles (θ) for different values of f_w, taking G_r=5.0, G_m=2.0, M=1.0, P_m=1.0, S_o =2.0, S_c=0.6 and E_c=0.2 as fixed.

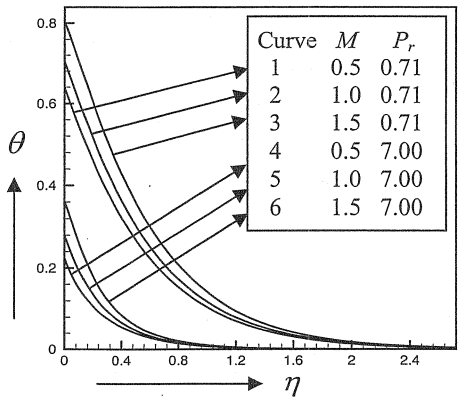

Fig. 18. Temperature profiles (θ) for different values of M, taking, f_w=2.0, G_r=5.0, G_m=2.0, P_m=1.0, S_o =2.0, S_c=0.6 and E_c=0.2 as fixed.

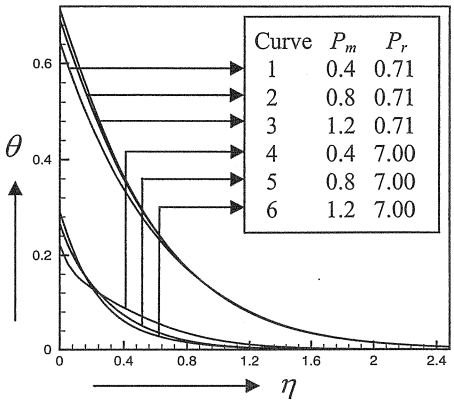

Fig. 19. Temperature profiles (θ) for different values of P_m, taking f_w=2.0 , G_r=5.0, G_m=2.0, M=1.0, S_o =2.0, S_c=0.6 and E_c=0.2 as fixed.

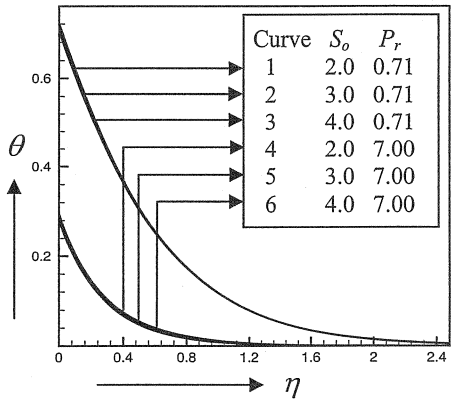

Fig. 20. Temperature profiles (θ) for different values of S_o, taking f_w=2.0 , G_r=5.0, G_m=2.0, M=1.0, P_m=1.0, S_c=0.6 and E_c=0.2 as fixed.

The displayed Figs. (22)-(26) show the effect of the various parameters f_w, M, P_m, S_o and E_c on the concentration field for both air (P_r=0.71) and water (P_r=7.0). From Fig.(22), it is observed that the concentration decreases with increase of the suction parameter (f_w) for both air and water. It is observed from Fig.(23) that a minor decreasing effect of concentration occurs within the interval $0<\eta<0.22$ (approx.) and

further it has a minor increasing effect from $\eta > 0.22$ in case of air, whereas for water the minor decreasing effect of concentration occurs in the interval $0 < \eta < 0.55$ (approx.) with increase in M. From Fig.(24), it is seen that the concentration has a minor increasing effect with increase in magnetic diffusivity parameter (P_m), while from Fig.(25), it is observed that the concentration increases close to the plate with the increase in Soret number (S_o). The decreasing effect of concentration is found in the interval $0 < \eta < 0.2$ for air and in $0 < \eta < 0.5$ for water (approximately), after that interval the effect is reversed with increase in E_c [Fig. (25)]. It should be pointed out the that in all Figs.(22)-(26), the concentration distributions are more sensitive for water (P_r=7.00) than for air (P_r=0.71) near to the wall up to a certain point, thereafter they are reversed.

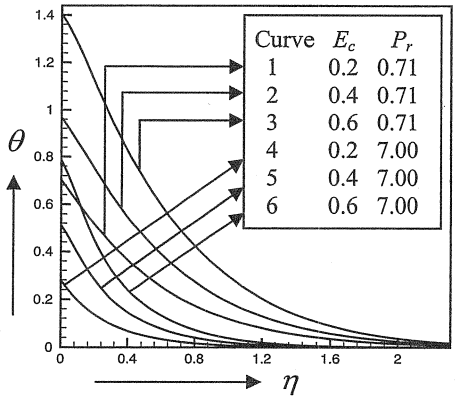

Fig. 21. Temperature profiles (θ) for different values of E_c, taking f_w=2.0, G_r=5.0, G_m=2.0, M=1.0, P_m=1.0, S_o =2.0 and S_c=0.6 as fixed.

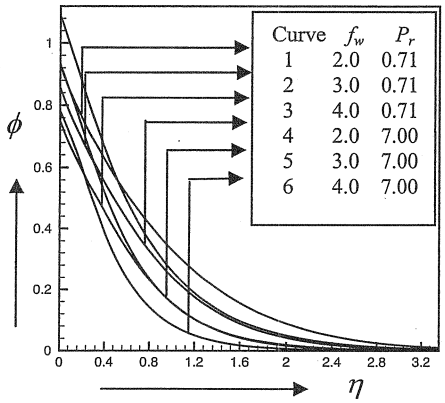

Fig. 22. Concentration profiles (ϕ) for different values of f_w , taking G_r=5.0, G_m=2.0, M=1.0, P_m=1.0, S_o =2.0, S_c=0.6 and E_c=0.2 as fixed.

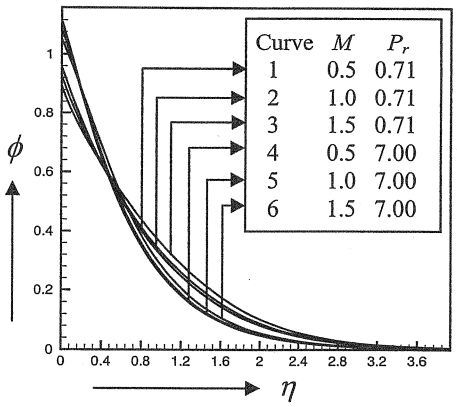

Fig. 23. Concentration profiles (ϕ) for different values of M, taking f_w=2.0, G_r=5.0, G_m=2.0, P_m=1.0, S_o =2.0, S_c=0.6 and E_c=0.2 as fixed.

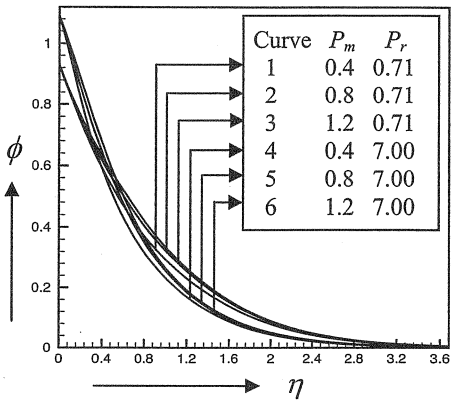

Fig. 24 Concentration profiles (ϕ) for different values of P_m, taking f_w=2.0 , G_r=5.0, G_m=2.0, M=1.0, S_o =2.0, S_c=0.6 and E_c=0.2 as fixed.

Finally, the effects of various parameters on the skin friction (τ) and the current density at the plate (J_w) are tabulated in Tables 1-5. It is observed from Table 1 that the skin friction (τ) decreases while the current density at the plate (J_w) increases with the increase of f_w for both air (P_r=0.71) and water (P_r=7.00). Tables 2-5 show that the skin friction and the current density at

the plate increases increases of M, P_m, S_o and E_c, respectively, for both air and water.

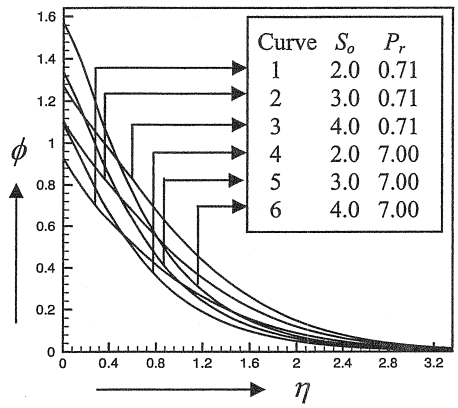

Fig. 25. Concentration profiles (ϕ) for different values of S_o, taking f_w=2.0 , G_r=5.0, G_m=2.0, M=1.0, P_m=1.0, S_c=0.6 and E_c=0.2 as fixed.

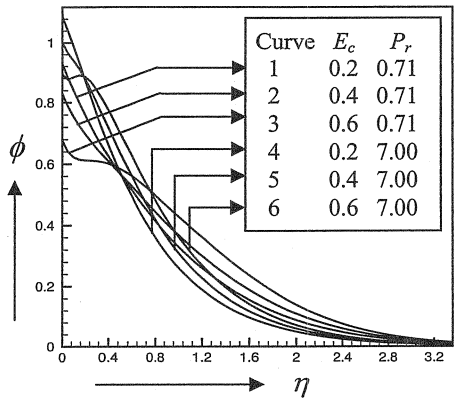

Fig. 26. Concentration profiles (ϕ) for different values of E_c, taking f_w=2.0, G_r=5.0, G_m=2.0, M=1.0, P_m=1.0, S_o =2.0 and S_c=0.6 as fixed.

Table 1. Numerical values of Skin friction (τ) and Current density at the plate (J_w) proportional to f'' and $-H'$, respectively, for different values of f_w , taking G_r=5.0, G_m=2.0, M=1.0, P_m=1.0, S_0=2.0, S_c=0.6 and E_c=0.2 as fixed.

P_r	f_w	f''	$-H'$
0.71	2.00	1.7504487	3.1397836
0.71	3.00	0.1334494	4.0073649
0.71	4.00	-0.3793490	4.9760911
7.00	2.00	0.3756603	3.0252324
7.00	3.00	-0.9692224	3.9721669
7.00	4.00	-2.2420256	4.9636363

Table 2. Numerical values of Skin friction (τ) and Current density at the plate (J_w) proportional to f'' and $-H'$ respectively, for different values of M, taking f_w=2.0, G_r=5.0, G_m=2.0, P_m=1.0, S_0=2.0, S_c=0.6 and E_c=0.2 as fixed.

P_r	M	f''	$-H'$
0.71	0.5	1.0777935	2.5055471
0.71	1.0	1.7504487	3.1397836
0.71	1.5	2.6215367	3.7948535
7.00	0.5	-0.1790336	2.4482994
7.00	1.0	0.3756603	3.0252324
7.00	1.5	1.0341457	3.6093244

Table 3. Numerical values of Skin friction (τ) and Current density at the plate (J_w) proportional to f'' and $-H'$ respectively, for different values of P_m, taking f_w=2.0, G_r=5.0, G_m=2.0, M=1.0, S_0=2.0, S_c=0.6 and E_c=0.2 as fixed.

P_r	P_m	f''	$-H'$
0.71	0.4	1.4363195	1.1319077
0.71	0.8	1.6810228	2.4725643
0.71	1.2	1.7993199	3.8003870
7.00	0.4	0.2051305	1.1183955
7.00	0.8	0.3347863	2.3866975
7.00	1.2	0.4061518	3.6616874

Table 4. Numerical values of Skin friction (τ) and Current density at the plate (J_w) proportional to f'' and $-H'$ respectively, for different values of S_0, taking f_w=2.0, G_r=5.0, G_m=2.0, M=1.0, P_m=1.0, S_c=0.6 and E_c=0.2 as fixed.

P_r	S_0	f''	$-H'$
0.71	2.0	1.7504487	3.1397836
0.71	3.0	2.1243856	3.1805336
0.71	4.0	2.4795386	3.2204364
7.00	2.0	0.3756603	3.0252324
7.00	3.0	0.7289248	3.0495142
7.00	4.0	1.0655068	3.0735690

Table 5. Numerical values of Skin friction (τ) and Current density at the plate (J_w) proportional to f'' and $-H'$ respectively, for different values of E_c, taking f_w=2.0, G_r=5.0, G_m=2.0, M=1.0, P_m=1.0, S_0=2.0 and S_c=0.6 as fixed.

P_r	E_c	f''	$-H'$
0.71	0.2	1.7504487	3.1397836
0.71	0.4	2.5692719	3.2191873
0.71	0.6	3.8088607	3.3484654
7.00	0.2	0.3756603	3.0252324
7.00	0.4	0.8479453	3.0518631
7.00	0.6	1.3962218	3.0861721

Nomenclature

x,y = Cartesian coordinates along the plate and normal to it
u,v = velocity components in x and y directions
U_0 = free stream velocity
T = fluid temperature within the boundary layer
T_∞ = fluid temperature in the free stream
C = concentration inside the boundary layer
C_∞ = concentration outside the boundary layer
H = induced magnetic field
J = current density
J_w = current density at the wall
f' = dimensionless velocity
f_w = suction parameter
H_0 = applied constant magnetic field
H_x = x-component of induced magnetic field
H_w = induced magnetic field at the plate
q = constant heat flux per unit area
m = constant mass flux per unit area
g = acceleration due to gravity
C_p = specific heat at constant pressure
T_m = mean fluid temperature
K_T = thermal diffusion ratio
D_m = coefficient of mass diffusion
k = the thermal conductivity
G_r = Grashof number
G_m = Modified Grashof number
M = magnetic force number
P_m = magnetic diffusivity parameter
P_r = Prandtl number
E_c = Eckert number
S_0 = Soret number
S_c = Schmidt number

Greek Symbols:

μ_e = magnetic permeability
ν = kinematic viscosity
ρ = fluid density
τ = skin friction
β = coefficient of thermal expansion
β^* = coefficient of mass expansion
σ' = electric conductivity
η = similarity variable
θ = dimensionless temperature
ϕ = dimensionless concentration

7. References

[1] Georgantopoulos G. A., Effects of Free Convection on the Hydromagnetic Accelerated Flow Past a Vertical Porous Limiting Surface, Astrophysics and Space Science, Vol.65, pp. 433-441, 1979.

[2] Nanousis N., Georgantopoulos G. A. and Papaioannou A., Hydromagnetic Free Convection Flow in the Stokes Problem for a Porous Vertical Limiting Surface with Constant Suction, Astrophysics and Space Science, Vol.70, pp. 377-383, 1980.

[3] Raptis A. and Singh A. K., MHD Free Convection Flow Past an Accelerated Vertical Plate, Int. Comm. in Heat and Mass Trans., Vol.10(4), pp. 313-321, 1983.

[4] Kafoussias N. G., Nanousis N. and Georgantopoulos G. A., Free Convection Effects on the Stokes Problem for an Infinite Vertical Limiting Surface with Constant Suction, Astrophysics and Space Science, Vol.64, pp.391-399, 1979.

[5] Singh A. K., MHD Free Convection Flow in the Stokes Problem for a Porous Vertical Plate, Astrophysics and Space Science, Vol. 87, pp.455-461, 1982.

[6] Singh A. K., Singh Aj. K. and Singh N. P., Hydromagnetic Heat and Mass Transfer in a Flow of a Viscous Incompressible Fluid Past an Infinite Vertical Porous Plate under Oscillatory Suction Velocity Normal to the Plate, Indian J. of Pure and Appl. Math., Vol.34, pp. 429-434, 2003.

[7] Chen C. H., Combined Heat and Mass Transfer in MHD Free Convection from a Vertical Surface with Ohmic Heating and Viscous Dissipation, Int. J. of Eng. Sci., Vol. 42(7), pp. 699-713, 2004.

[8] Sakiadis B. C., Boundary-layer Behavior on Continuous Solid Surfaces: I. Boundary-

layer Equations for Two-dimensional and Axisymmetric Flow, AIChE J., Vol.7, pp. 26-28,1961.

[9] Sakiadis B. C., Boundary-layer Behavior on Continuous Solid Surfaces: II. The Boundary Layer on a Continuous at Surface, AIChE J., Vol.7 , pp. 221-225, 1961.

[10] Soundalgekar V. M., Ramana Murty T.V., Heat Transfer in Flow Past a Continuous Moving Plate with Variable Temperature, Warme, Stoffubertrag, Vol. 14, pp. 91-93, 1980.

[11] Al-Sanea S. A., Mixed Convection Heat Transfer Along a Continuously Moving Heated Vertical Plate with Suction or Injection, Int. J. of Heat Mass Trans., Vol. 47, pp.1445-1465, 2004.

[12] Chaudhary R. C. and Sharma B. K., Combined Heat and Mass Mransfer by Laminar Mixed Convection Flow from a Vertical Surface with Induced Magnetic Field, J. of Appl. Phys., Vol. 99, pp. 034901-10, 2006.

[13] Eckert E. R. G. and Drake R. M., Analysis of Heat and Mass Transfer, McGraw-Hill Book Co., New York, 1972.

[14] Kafoussias N. G., MHD Thermal-diffusion Effects on Free-convective and Mass-transfer Flow over an Infinite Vertical Moving Plate, Astrophysics and Space Science, Vol.192, pp. 11-19, 1992.

[15] Nanousis N., Thermal-diffusion Effects on MHD Free Convective and Mass Transfer Flow Past a Moving Infinite Vertical Plate in a Rotating System, Astrophysics and Space Science, Vol.191, pp.313-322, 1992.

[16] Sattar M. A. and Alam M. M., Thermal-Diffusion as well as Transpiration Effects on MHD free Convection and Mass Transfer Flow Past an Accelerated Vertical Porous Plate, Indian J. of Pure and Appl. Math., Vol.25(6), pp. 679-688,1994.

[17] Alam M. S., Rahman M. M., Samad M.A., Dufour and Soret Effects on Unsteady MHD Free Convection and Mass transfer Flow Past a Vertical Porous Medium, Nonlinear Analysis: Modelling and Control, Vol.11(3), pp. 217-226, 2006

[18] Alam M. S. and Rahman M. M., Dufour and Soret Effects on Mixed Convection Flow Past a Vertical Porous Flat Plate with Variable Suction, Nonlinear Analysis: Modelling and Control, Vol.11(1), pp.3-12, 2006.

[19] Nachtsheim P. R. and Swigert P., Satisfaction of the Asymptotic Boundary Conditions in Numerical Solution of the System of Non-linear Equations of Boundary Layer Type. NASA TND-3004., 1965.